ANALYSIS OF THE INTERACTION BETWEEN GABAA RECEPTOR AND L-TRIIODOTHYRONINE USING ELECTROPHYSIOLOGY AND MOLECULAR DYNAMICS SIMULATIONS

By

THOMAS WESTERGARD

A thesis submitted to the

Graduate School-Camden

Rutgers, The State University of New Jersey

in partial fulfillment of the requirements

for the degree of

Master of Science

Graduate Program in Computation and Integrative Biology

written under the direction of

Joseph Martin and Grace Brannigan

and approved by

_____

Joseph Martin

_____

Grace Brannigan

_____

Patrick McIlroy

Camden, New Jersey

May, 2013

ABSTRACT OF THE THESIS

Analysis of the interactions between $GABA_A$ receptor and L-triiodothyronine using electrophysiology and molecular dynamics simulations

By THOMAS WESTERGARD

Thesis Directors:

Grace Brannigan and Joseph Martin

Disorders of the thyroid cause a multitude of neurological dysfunctions including depression, anxiety, and psychosis. Thyroid hormones have been primarily thought to act via genomic mechanisms throughout the organism; however, another mechanism has been proposed for the adult brain. Functional experiments on expressed recombinant $GABA_A$ receptors demonstrated a rapid inhibition of GABA responses in the presence of the thyroid hormone triiodothyronine (T3), and, at much higher concentrations of T3 alone, a direct stimulation of receptor activity. We hypothesize that T3 acts directly on $GABA_A$ receptors via a mechanism similar to that of neurosteroids. To determine this mechanism of T3, competition studies with T3 against molecules with known binding motifs (ivermectin) were investigated utilizing two-electrode voltage-clamp measurements of the $\alpha1\beta1\gamma2$ $GABA_A$ receptor expressed in *Xenopus* oocytes. T3 inhibited ivermectin in a competitive manner, with a Schild plot slope of 1.27 ± 0.03 and

no significant difference from unity. All atom molecular dynamics were employed to analyze the possible interaction of T3 and the $GABA_A$ receptor (based on the crystal structure of the related glutamate-gated chloride channel). In simulations, T3 stabilizes in the transmembrane domain of the $GABA_A$ receptor in a region that is associated with the activation by neurosteroids. Our results provide strong evidence supporting earlier experimental findings indicating a role of T3 in regulating the activity of $GABA_A$ receptors in brain.

ACKNOWLEDGEMENT

I would like to first thank my mentors Dr. Grace Brannigan and Dr. Joseph Martin. Their combined guidance encouraged critical thinking and excellence in research. They have both motivated the best research and student that I can possibly be. They were very supportive and easy to converse with, and I consider myself fortunate to be both their student.

Steve Moffett is a great friend and highly knowledgeable lab partner. He was always there to bounce ideas off and assist anytime I needed help.

Tom James was a former lab partner and friend. He helped with the initial understanding and experimental work for my project.

Jerome Henin, Reza Salari, Ruchi Lohia, and Sruthi Murlidaran who all helped with the molecular dynamics aspect of my research.

I would also like to thank Dr. Patrick McIlroy, a member of my committee. He has always been a very zealous, friendly, and knowledgeable faculty who has helped me in both my research and education.

DEDICATION

I would like to dedicate this work to my family and friends who supported me along the way.

TABLE OF CONTENTS

LIST OF FIGURES

INTRODUCTION

The neurotransmitter γ-aminobutyric acid (GABA) is the primary inhibitory modulator in the central nervous system. The neurotransmitter acts primarily on the ionotropic $GABA_A$ receptor, a chloride channel that is part of the Cys-loop ligand gated ion channel superfamily. When GABA binds to this receptor, the channel becomes stable in the open conformation, allowing chloride to flow into the cell and, in most cases, causing hyperpolarization. As part of the Cys-loop family, the $GABA_A$ receptor is characterized by a pentameric arrangement of subunits around a central pore; each subunit is composed of one of 19 species (α_{1-6}, β_{1-3}, γ_{1-3}, δ, ε, π, θ, ρ_{1-3}). While there are a multitude of combinations in order and type of these subunits, not all are functional combinations (Baumann et al, 2002). Variation in subunits allows for differing allosteric binding sites (Hill-Venning et al, 1997), where a multitude of substances can modulate the effects of GABA and can even directly activate the receptor. Drugs like anesthetics (Krasowski and Harrison, 1999) and sedatives (Rudolph and Möhler, 2006) potentiate GABA's effect or directly gate the receptor, enhancing inhibition of cellular activity. Additionally, the effects of GABA have been shown to be modulated by substances known as neurosteroids, locally synthesized steroids that act as endogenous sedatives and anesthetics (Lambert et al, 2009).

The thyroid hormone, triiodothyronine (T3), has also been shown in functional studies to modulate the $GABA_A$ receptor. In the presence of GABA, T3 inhibits the activity of GABA gated chloride currents on recombinant $GABA_A$ receptors expressed in human embryonic kidney-293 cells and *Xenopus* oocytes (Martin et al, 1996; Chapell et

al, 1998). Uniquely, however, T3 alone in higher concentrations will activate the receptor, causing a chloride influx (Chapell et al, 1998). The rapid *in vitro* effects of T3 in these studies are support of a non-genomic action of T3. A neurotransmitter-like mechanism of thyroid hormone action had been previously proposed based on presynaptic localization of T3 (Mason et al, 1993; Dratman and Gordon, 1996). T3 inhibition on GABA gated chloride currents was determined as non-competitive through the binding site of GABA (Chapell et al, 1998). This suggests that there is direct interaction of T3 with the $GABA_A$ receptor in some allosteric binding site.

Unfortunately, when comparing T3 to other GABA modulators, the mechanism of action for T3 is unclear. Assortments of compounds potentiate the $GABA_A$ receptor at low concentrations, while directly opening the receptor at higher concentrations. Propofol (Hara et al, 1993), and pentobarbital (Peters et al, 1988), as well as the neurosteriods allopregnanolone (Puia et al, 1990) and alphalaxone (Barker et al, 1987), all directly activate the $GABA_A$ receptor. However, low doses of T3 inhibit instead of potentiating the $GABA_A$ receptor. The inhibiting effect on $GABA_A$ receptors is seen in compounds like pregnenolone sulfate (Akk et al, 2001) and dehydro-epiandrosterone, DHEA (Park-Chung et al, 1999), but neither of these directly activates the channel. Typical modulatory and direct gating of modulators are in the nanomolar and micromolar concentrations, but the effects of T3 all occur at the micromolar concentrations (Chapell et al, 1998).

An incomplete knowledge of the structure of the $GABA_A$ receptor prevented understanding the mechanism of action behind allosteric modulators of the receptor. Previous research with other Cys-loop receptors has indicated possible mechanisms, but these studies focused on cationic and mostly prokaryotic receptors (Hilf and Dutzler,

2008; Hilf and Dutzler 2009; Boquet et al 2009). Recently, however, a high-resolution crystal structure for the anionic glutamate-gated chloride channel (GluCl) was established from *C. elegans* (Hibbs and Gouaux, 2011). The crystal structure represents the receptor in the open state with the molecule ivermectin bound at the subunit interface in the transmembrane domain. The GluCl and the $GABA_A$ receptor are both anionic Cys-loop receptors, have a high similarity in structure of subunits (46% identity in the transmembrane domain), and are activated by ivermectin (Adelsberg et al, 1997; Adelsberg et al, 2000; Arena,1994; Martin et al., 1997; Krsek and Zemkov, 1994). Using the GluCl as a template, a functional homology model of the $GABA_A$ receptor can be produced for molecular dynamics.

The transmembrane domain of the $GABA_A$ receptor model is characterized by four alpha helical domains for each subunit (referred to as M1 – M4). The M2 alpha helices structure the pore of the receptor, containing leucine amino acid residues that compose a hydrophobic constriction for ions passing through. Ivermectin is wedged and inserted deeply between the M3 alpha helix of one subunit and the M1 alpha helix of the adjacent subunit, making significant contacts with serine residues of the M2 alpha helix. This transmembrane location of ivermectin has been indicated to be a possible binding site for neurosteroids (Hosie et al, 2006). Parallels between T3 and neurosteroids in molecular dimensions and functional groups (Fig. 1), synthesis in the central nervous system (Bauleiu, 1991; Gee, 1988; Majewska, 1992; Purdy et al, 1990; Dratman and Crutchfield, 1976, Dratman et al, 1983; Tanaka et al, 1981), and alteration of ligand binding (Gee et al, 1988; Majewska et al, 1986; Simmonds et al, 1983; Go et al, 1988; Kragie, 1993; Medina and DeRobertis, 1985; Nagy and Lajtha, 1983; Narihara et al,

1994) suggests a neurosteroid-type mechanism in the ivermectin transmembrane domain may be probable for T3. A possible "wedge" mechanism of action has been suggested for ivermectin (Hibbs and Gouaux, 2011), implying a potentially similar mechanism for T3.

Our current study uses two-electrode voltage-clamp recordings and molecular dynamics simulations to explore this potential binding site for T3. Our studies used the $\alpha1\beta1\gamma2$ $GABA_A$ receptor construct, a common functional construct, which is comparable to the $\alpha1\beta2\gamma2$ $GABA_A$ receptor as the beta subunit does not influence neurosteroid effects (Belelli et al, 2002). Through two-electrode voltage-clamp measurements of the $\alpha1\beta1\gamma2$ $GABA_A$ receptor expressed in *Xenopus* oocytes, we further study the interaction between T3 and positive modulators, like ivermectin. Competitive binding studies and a Schild plot analysis was performed with T3 against these modulators with known binding motifs to determine a possible binding site.

Molecular dynamics simulations can reveal potential interactions between T3 and the $GABA_A$ receptor. The homology model for the $GABA_A$ receptor of $\alpha1\beta1\gamma2$ was in the order of $\gamma2\alpha1\beta1\alpha1\beta1$ clockwise and T3 was aligned to the ivermectin molecule. T3 also contains two polar groups at each end, suggesting that either end could hydrogen bond with buried serine residues thought to be essential for modulation. To determine the most probable alignment for T3, a docking analysis was performed. The simulations were analyzed against control and cholesterol-bound simulations run and analyzed in previous studies. A possible "wedge" mechanism similar to ivermectin was analyzed as a possible mechanism for the action of T3.

MATERIALS AND METHODS

Materials

GABA, ivermectin, T3, and all other materials unless stated otherwise were obtained from Sigma (St. Louis, MO). T3 was dissolved in 0.1 M NaOH to make a stock concentrate of 1 mM T3. During trials involving ivermectin, all solutions were dissolved in no more that 5% v/v dimethyl sulphoxide (DMSO) due to the low solubility of the substances. This concentration of DMSO had no effect on the membrane properties of the oocytes.

The cDNAs encoding human GABAA receptor subunits were acquired from ATCC (Manassas, Virginia). Restriction enzymes for the cDNAs came from New England Biolabs (Ipswich, MA).

Xenopus laevis were obtained from Xenopus Express Inc (Brooksville, FL). *X. laevis* were maintained according to Rutgers University Animal Care standards. The experimentation was approved by the Institutional Animal Care and Use Committee at Rutgers University.

Synthesis of cRNAs

HindIII-digested and *XholI*-digested DNA templates encoding human $GABA_A$ receptor subunits (4 μg) were transcribed through the mMESSAGE mMACHINE T7 kit from Ambion (Austin, TX). The solution was then treated with RNase-free DNase I and precipitated with lithium chloride. The cRNAs were dissolved in double-distilled diethyl-pyrocarbonate (DEPC) treated water to a final concentration of ~ 1-2 μg/ μl. Subunit

combinations were alioquoted for specific receptor type with total concentration remaining ~ 1-2 μg/ μl.

Oocyte preparation

X. laevis were anesthetized by placing them in solution of 1g MS222 per 500 ml in de-chlorinated water. A small incision in the abdomen was made 1 cm parallel of the midline and lobes of ovary were removed. The lobes were gently agitated at room temperature with collagenase (2 mg/ml) in calcium free OR-2 (82.5 mM NaCl, 2.5 mM KCl, 1 mM $MgCl_2$, 5 mM HEPES, pH adjusted to 7.6 with NaOH) until the ovarian epithelium and the follicular cell layer were dissolved (~2 hrs). Oocytes were checked for proper size and shape, color, and for the presence of distinct animal and vegetal poles. Viable oocytes were placed in ND96 solution (96 mM NaCl, 2mM KCl, 1 mM $MgCl_2$, 1 mM $CaCl_2$, 5 mM HEPES, pH adjusted to 7.6 with NaOH) and the oocytes were injected with 46 nL cRNAs (1-2 μg/ μl) expressing the $\alpha_1\beta_1\gamma_2$ construct using a digital microdispenser (Drummond 'Nanoject II'). Injected oocytes were incubated at 18ºC in a sterile medium containing Leibovitz L-15 Medium supplemented with .01M HEPES, Gentamicin and Tetracycline pH 7.4.

Two-electrode voltage-clamp recording

After 24hrs following injections, oocytes were placed in the recording chamber perfused continually with ND96. All drugs were perfused into the chamber through a gravity flow system (~5 ml/min). Oocytes were impaled with two 3 M KCl-filled glass microelectrodes (~ 1-2 MΩ). Oocytes were then voltage clamped at -60 mV with a Model OC-725C Oocyte Clamp (Warner Instruments, Hamden, CT). Currents were recorded

using the iWorx LabScribe v1.959 software. Peak amplitudes of responses were used for data. Graph Pad Prism was use for all statistical analysis and determinations of EC_{50}/IC_{50}.

Trials began after five consecutive GABA or ivermectin responses were observed to allow for the peak amplitude of response to be established. In trials with T3, oocytes were preincubated with T3 (1-100 μM) for 20 s, followed directly with coapplication of T3 and GABA or ivermectin as previous protocols suggest (Chapell et al, 1998). The responses are expressed as percent of the peak amplitude of response previously determined.

To determine the effects of T3 on the response of GABA or ivermectin, oocytes were perfused with 10 μM of GABA or ivermectin in the presence of varying T3 concentrations (0-100 μM). The peak responses were taken as a percentage of the maximum response in the presence of no T3.

During the competitive binding studies, concentration-response curves of GABA or ivermectin (0.1 – 125 μM) were determined in steady concentrations of T3 (0 – 20 μM). Pre-trial response of 125 μM GABA or ivermectin without T3 was used as the maximum response values were compared to.

Molecular dynamics system setup

Simulations used a previous built model of the $GABA_A$ receptor, constructed using the alignment in Hibbs and Gouaux, 2011 and the structure for the glutamate-gated chloride channel from *C. Elegans* (PDB code:3RHW) as a template. The $\alpha_1\beta_1\gamma_2$ $GABA_A$ receptor construct was assembled and aligned in the order of $\gamma_2\alpha_1\beta_1\alpha_1\beta_1$ (clockwise).

T3 was docked to the $GABA_A$ model by alignment with the ivermectin present in the GluCl model using VMD (Humphrey et al, 1996). Docking analysis utilizing

AutoDock Vina (Trott and Olson, 2010) was used to determine the most probable alignment of T3 to ivermectin. The $GABA_A$ receptor and T3 were placed into a 12 x 12 nm^2 lipid bilayer with a 3 to 1 concentration of 1-palmitoyl-2-oleoyl-sn-glycerol-phosphatidyl-coline (POPC) and cholesterol using VMD (Humphrey et al, 1996). The system was fully solvated to a box size of 12 x 12 x 18 nm^3 using Solvate (Grubmüller et al, 1996), and ionized with sodium and chloride ions for a 0.15 M solution to neutralize the system.

Running the simulation

All simulations were run using the NAMD2.9 package (Phillips et al, 2005). The CHARMM22-CMAP force field was used for proteins (MacKerell et al, 2004) and CHARMM36 was used for the phospholipids, ions, and water (Smart et al, 1996). Periodic boundary conditions were applied, with particle-mesh Ewald long-range electrostatics and a cut-off of 1.2 nm Lennard-Jones potentials, with a smooth switching function starting at 1.0 nm. The simulations were run at a temperature of 300 K and pressure of 1 atm. Simulations started with 5 ns of simulation with harmonic restraints on the protein. The restraints were then lifted and the simulation ran for another 195 ns. All MD runs were performed on the Cray XT5 supercomputer Kraken at the National Institute for Computational Sciences, University of Tennessee at Knoxville, Tn.

Analysis of data

Two-electrode voltage-clamp measurements were plotted and analyzed using Graph Pad Prism. Measurements were fit with a non-linear fit dose-response curve to acquire IC/EC50 values, min and max response values, and Hill coefficients. To determine type of competition, a Schild plot analysis utilizing a linear regression fit was

applied to the competitive binding data. The ivermectin dose response EC50 values at various T3 concentrations were compared to the EC50 value with no T3 present, and then plotted against the log concentration of T3. The slope and x-intercept were used to analyze the type of competition and possible KD of T3.

A frame-by-frame analysis was performed for the simulations using scripts that utilized functions in the software VMD (Humphrey et al, 1996). The analysis measured root-mean-squared deviations (RMSD), pore radius, and tilt of transmembrane helices. Pore radius was measured using HOLE (Smart et all, 1996). To test the possibility of a "wedge"-like mechanism of action, distances between M1 and M3 helices were also measured.

RESULTS

Inhibition of GABA response by T3 on the α1β1γ2 $GABA_A$ construct

The effect of T3 (0.1 μM- 100 μM) on GABA (10 μM) response was characterized on *Xenopus* oocytes expressing α1β1γ2 constructs (Fig. 2). A representative trace shows a significant reduction in the response of GABA in the presence of 10 μM T3 (Fig. 2A). The response of GABA was reduced in the presence of T3 to 59.7% ± 3.0% of control. The IC50 of T3 was 8.3 ± 2.2 μM (Fig. 2B). A near-maximal effect of T3 appears to be demonstrated between 50 – 100 μM T3.

Activation of ivermectin and the inhibition of response by T3 on the α1β1γ2 $GABA_A$ construct

A dose response curve characterized the effect of ivermectin (0.1 μM – 125 μM) on *Xenopus* oocytes expressing α1β1γ2 constructs (Fig. 3). No effect of ivermectin on uninjected oocytes was observed (not shown). A maximum effect of ivermectin appears to be between 20 – 50 μM with an EC50 of 7.07 ± 0.8 μM. The Hill coefficient was calculated to be 1.88 ± 0.4 indicating two agonist-binding sites.

To determine a possible inhibition of invermectin by T3, the effect of T3 (0.1 μM- 100 μM) on the ivermectin (10 μM) response was characterized on *Xenopus* oocytes expressing α1β1γ2 constructs (Fig. 4). A representative tracing shows a significant reduction in the response of ivermectn in the presence of 10 μM T3 (Fig. 4A). The response of ivermectin was reduced in the presence of T3 to 51.2% ± 5% of control. The IC50 of T3 was 7.2 ± 2.5 μM (Fig. 4B). A near-maximal effect of T3 appears to be demonstrated around 50 μM T3.

Competition binding study of T3 against ivermectin

Dose response curves of ivermectin (0.1 μM – 125 μM) were constructed in various steady concentrations of T3 (0-20 μM) to determine the type of inhibition T3 exerted on ivermectin (Fig. 5). Increasing concentrations of T3 shifted curves to the right increasing IC50 values. No changes were observed in the maximum response. A Schild analysis was performed on the dose response curves to determine type of inhibition (Fig. 6). The dose responses with T3 were compared to the dose response in the absence of T3. The log of this value was subtracted by 1 and plotted against the log concentration of T3. The slope of the Schild analysis was 1.20 ± 0.08 with no significant difference from unity (slope of 1). A pA2 value of -5.031 ± .48 log concentration of T3 was calculated, indicating a possible measurement of affinity of T3 to the $GABA_A$ receptor.

Molecular dynamics simulations demonstrating the interaction of T3 on the α1β1γ2 $GABA_A$ construct

Docking software confirmed the possible binding site for T3 at the site where Ivermectin was bound (Fig. 7). The docking analysis yielded one primary orientation for T3, with the amino acid group arranged towards the pore, which was used for simulations.

Molecular dynamics simulations suggest that T3 is stable in the intersubunit site between all subunits (Fig. 8). The simulations show a deep embedding of all T3 molecules in between the M3 and M1 of adjacent subunits in the transmembrane domain. Hydrogen bonding between T3 and the serine residue (Ser 265) of the M2 helix was visible throughout the simulation (Fig. 9).

Changes of pore profile through the interaction of T3 on the receptor

The pore radius was analyzed for changes caused by the presence of T3 and compared to a control with no ligand bound to the transmembrane domain site and a cholesterol-bound simulation. The pore size (averaged over frames) was calculated as a function of position along the longitudinal axis of the receptor (Fig. 10). The longitudinal axis represents the extracellular domain (positive value) to the transmembrane domain (more negative value), with 0 being the hydrophobic leucine constriction of the receptor. The minimum pore size was plotted along time, and a histogram of the data was taken (Fig. 11). These quantitative measurements display a pore radius distribution of a peak at ~ 2Å.

Changes in subunits through the interaction of T3 on the receptor

Root-mean-square deviations (RMSD) indicate motion of the receptor away from the initial coordinates. The RMSD plot shows the α and β subunits position away from their initial coordinates briefly and then remaining relatively stable at these coordinate (Fig. 12). The γ subunit, however, continues to have motion further away from its initial coordinates.

Analyzing the distance of the M1, M2, and M3 from the pore, as well as the distance between the M1-M3 in the same subunit and M3-M1 of adjacent subunits, reveals a possible “wedge”-like mechanism behind the action of T3. All helical distances from the pore increase with T3 versus the control (Fig 13). The intrasubunit distances between the M1-M3 remain significantly unchanged through time and are significantly similar to the control and cholesterol-bound, but the M3-M1 intersubunit distances significantly increase over time and are significantly larger than the control and

cholesterol-bound (Fig 14). The increase changes in intersubunit distances present with no changes in intrasubunit distances are consistent with a “wedge”-type mechanism.

The tilts of these helices can also elucidate some mechanisms of action. The radial tilt reflects tilt towards or away from the pore and tangential tilt reflects tilt tangent to the circle defined by M2 helices. All helical radial tilt values were higher with T3 than the control (Fig. 15A). This demonstrates a greater tilt away from the pore in the presence of T3. The tangential tilt values were lower in all helices with T3 than the control (Fig. 15B). Lower tangential tilt values exhibits less lateral movement of the helices in the presence of T3, consistent with a “wedge”-type mechanism.

DISCUSSION

Although the inhibitory effect of T3 on GABA has been previously described for a few constructs of the $GABA_A$ receptor, here we show the effects of T3 on GABA in the $\alpha1\beta1\gamma2$ $GABA_A$ construct (Martin et al, 1996; Chapell et al, 1998). T3 inhibits GABA induced chloride currents in *Xenopus* oocytes expressing the $\alpha1\beta1\gamma2$ $GABA_A$ construct. Interestingly, the inhibition of the GABA response by T3 on the $\alpha1\beta1\gamma2$ $GABA_A$ construct was highly similar to the inhibition characterized by T3 on the $\alpha1\beta2\gamma2$ $GABA_A$ construct (Chapell et al, 1998). Insensitivity to the β subunit is a characteristic of modulation by neurosteroids (Belelli et al, 2002), suggesting further analogy between the two classes of molecules.

To determine the binding site(s) and unique mechanism of action of T3, we used ivermectin as a potential binding site due to the known binding site in the transmembrane domain and direct gating effect on the $GABA_A$ receptor (Hosie et al, 2006; Adelsberger et al, 2000). While the activation of $GABA_A$ receptors by ivermectin described for the $\alpha1\beta2\gamma2s$ rat recombinant $GABA_A$ construct, here we report has similar results for the $\alpha1\beta1\gamma2$ $GABA_A$ construct (Adelsberger et al, 2000).

The possible inhibition of ivermectin activation by T3 was next characterized. We were able to show evidence of T3 inhibiting the direct gating effects of ivermectin. A competitive binding study was utilized to determine the type of inhibition that T3 was producing on ivermectin. We demonstrated right shifting EC50 values of ivermectin with no change in the maximum response of ivermectin, a characteristic exhibited by competitive inhibitors. A Schild plot confirmed the type of inhibition to be competitive,

as the slope did not significantly differ from unity. This evidence implies that the ivermectin transmembrane domain binding spot is also a binding site for T3.

Concurrently, we used molecular dynamics simulations to further support the possible binding site in this transmembrane domain as well as develop an understanding of the mechanism behind the action of T3 on the receptor. Our docking analysis showed that T3 at the subunit interface, with the amino acid end pointing towards the pore. By aligning T3 in this orientation to the ivermectin molecule, we were able to show T3 interacting with receptor throughout the 200 ns simulation. The T3 molecules embed between each subunit of the receptor and interact with various components of the subunit helices. The most notable interaction is the hydrogen bonding that occurs between T3 and the serine residues of the M2 helix of each subunit. This serine residue interaction has been noted to be important for ivermectin binding to the $GABA_A$ receptor (Hibbs and Gouaux, 2011). These results further strengthened the argument that this transmembrane subunit interface is a binding site for T3.

Analyzing the simulation gave us some insight onto the mechanism into which T3 alters the receptor in this binding site. The hydrophobic constriction that is made up of leucine residues is a key determinate in whether chloride ions can pass through the channel of this receptor. Our analysis shows that the radius of this gate is larger in the simulation with T3 than it is in the control simulation with no ligand present in any binding sites. However, the radius is still very similar to the size of cholesterol. A histogram of the profile of the gate's radius throughout the simulation reveals an overlapping distribution of the T3 and the control radius, but T3 has a large distribution that has a bigger radius than the control. Whether this is showing a closing or opening of

the pore really cannot be concluded, but what can be said is that T3 is altering the hydrophobic constriction and pore radius through some mechanism at this binding site.

To determine in what way T3 was altering the pore size, we looked at the possibility that T3 not only interacts with the serine residues, but acts as a physical "wedge" in between the subunits, altering the distance between the helices of the subunits. Our approach to determining this was to look at the changes in the M1 and M3 helices of subunits, where T3 is located in the transmembrane domain. We first saw that the distances of the M1, M2, and M3 helices from the pore for each subunit were increased with the interaction of T3. Next, we looked at the distances of the M1 and M3 of adjacent subunits as well as the distance between the M3 and M1 helices of the same subunit. The intersubunit distance of M1 and M3 of adjacent subunits significantly increased and was larger than the control simulations. The intrasubunit distances between the M3 and M1 did not significantly change and was not significantly larger than the control simulation. These findings are consistent with a physical "wedge"-type mechanism, giving us a better insight into how T3 is altering the pore.

Combining the information from both experimental approaches, electrophysiology and molecular dynamics, we develop a better understanding of where T3 binds, as well as the possible mechanism by which T3 affects this binding site. However, whether this binding site is a site where it modulates the effect of $GABA_A$ channel activators, where is directly activates the channel, or does both is difficult to determine through this experiment. Neither the simulations nor the competitive binding studies were in the presence of GABA, where T3 has primarily shown its modulatory behavior. The presence of GABA could affect the binding affinity of T3 for another site,

which would be more favorable and would cause the modulatory behavior of T3. The competitive binding study showed competitive inhibition of T3 at this site, but it is possible that T3 is acting as a partial agonist at this site. Partial agonists create a low agonistic effect and do appear as competitive inhibitors in the presence of stronger agonists. Separate binding sites for the modulatory and direct gating effects of T3 have been suggested before (Chapell et al, 1998). Through the β2γ2 $GABA_A$ construct, the modulatory behavior of T3 on the GABA response was diminished, but the direct gating effect remained. However, this can indicate subunit specificity for the effect of T3 in the transmembrane subunit interface.

The molecular dynamics simulations demonstrate T3 binding in between all subunits of the $GABA_A$ receptor. Most likely in a biological environment this would demonstrate high concentrations of T3, where the direct gating properties are more likely seen (Chapell et al, 1998). T3 bound between all subunits demonstrated symmetric binding in the $GABA_A$ receptor. Symmetric ligand binding has been implicated to cause differing effects versus asymmetric binding in pentameric ligand-gated ion channels (Mowrey et al, 2013).

While these possible mechanisms have yet to be determined through our experimentation, we have established a binding site for T3. The unique approach of using both electrophysiology and molecular dynamics techniques synergistically verified this binding site and helped revealed possible mechanism behind the action of T3. Further experiments using this approach can help further elucidate the distinctiveness of the effect of T3 and potentially reveal unique $GABA_A$ receptor functions yet to be understood.

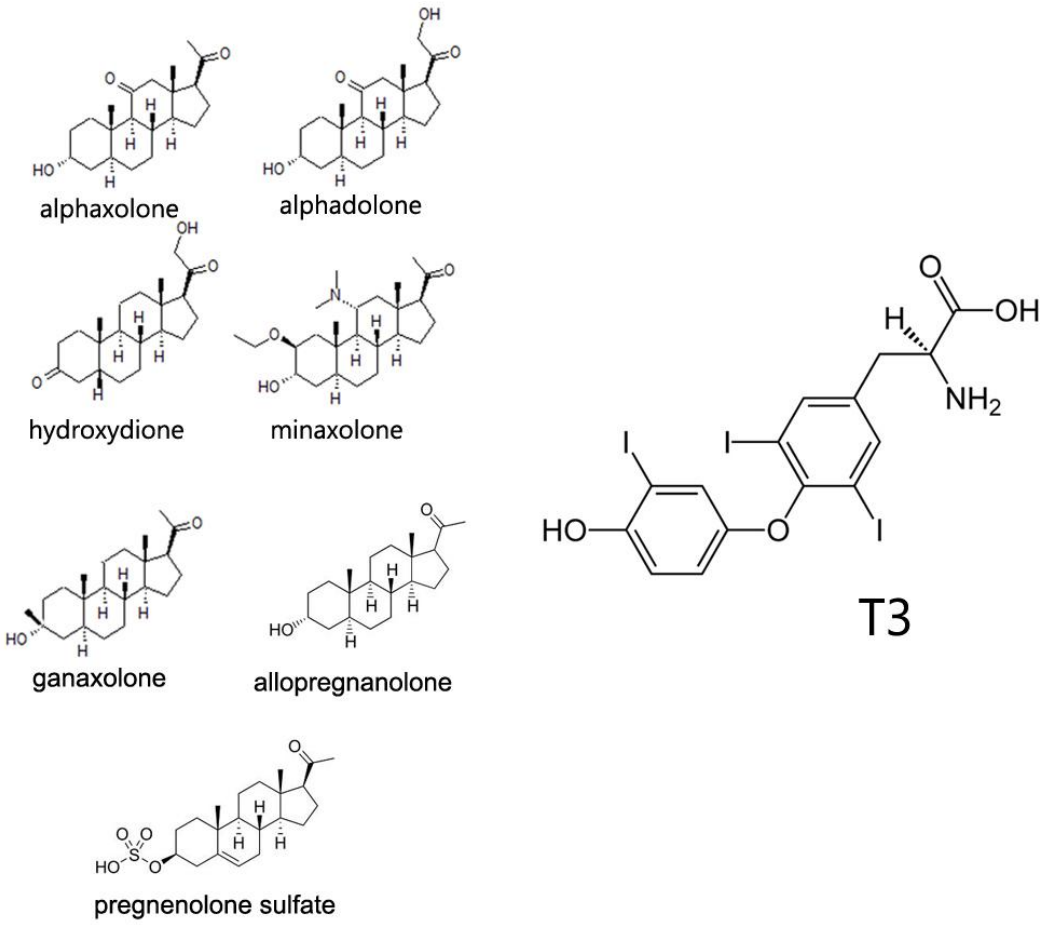

Figure 1. Comparison of T3 to neurosteroids. There are multiple similarities in molecular size and functional groups of T3 compare to neurosteroids.

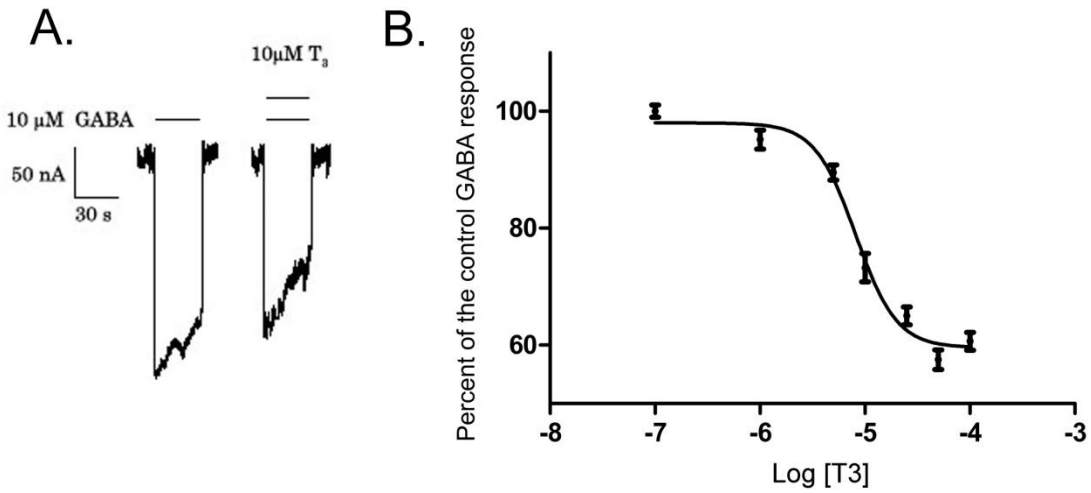

Figure 2. GABA response inhibited by T3. A. A representative tracing shows T3 inhibition on the GABA response in the α1β1γ2 $GABA_A$ construct. A significant change in response of GABA is seen in the presence of 10 µM T3. **B.** GABA (10 µM) was applied in various concentrations of T3 (0.1 µM – 100 µM). T3 inhibits the response with an IC50 of 8.3 ± 2.2 µM. Results are represented as a percentage of the maximal GABA response without T3 presence (mean ± S.E.M., n =3).

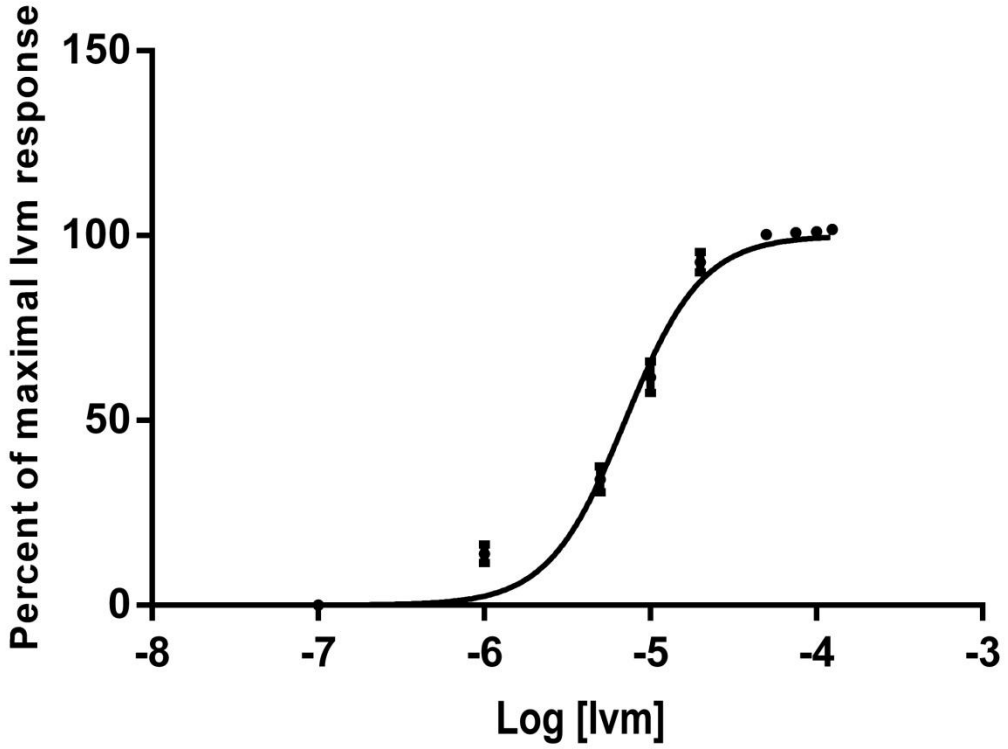

Figure 3. Ivermectin activation of the $GABA_A$ Receptor. Ivermectin concentration-response curves on the α1β1γ2 $GABA_A$ construct. Activation of the channel, increasing chloride influx was observed with an EC50 of 7.07 ± 0.8 μM and Hill coefficient of 1.88 ± 0.4. Results are represented as a percentage of the maximal ivermectin response at 125 μM (mean ± S.E.M., n =3).

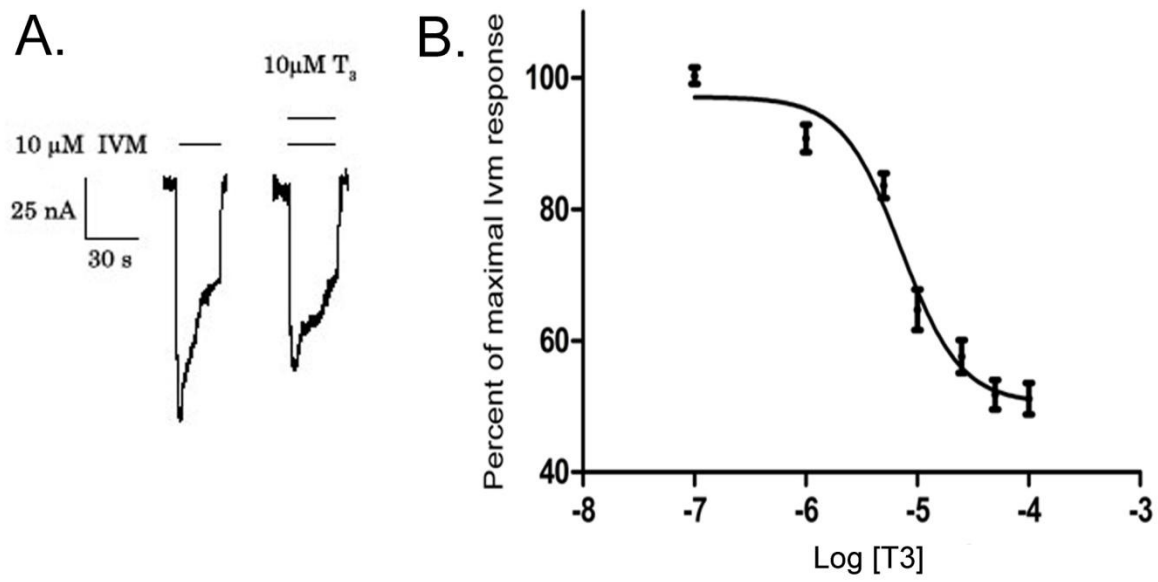

Figure 4. Ivermectin response inhibited by T3. A. Characterization of T3 inhibition on the ivermectin response in the α1β1γ2 $GABA_A$ construct. A significant change in response of ivermectin is seen in the presence of 10 µM T3. **B.** Ivermectin (10 µM) was applied in various concentrations of T3 (0.1 µM – 100 µM). T3 inhibits the response to ivermectin with an IC50 of 7.2 ± 2.5 µM. Results are represented as a percentage of the maximal ivermectin response without T3 presence (mean ± S.E.M., n =3).

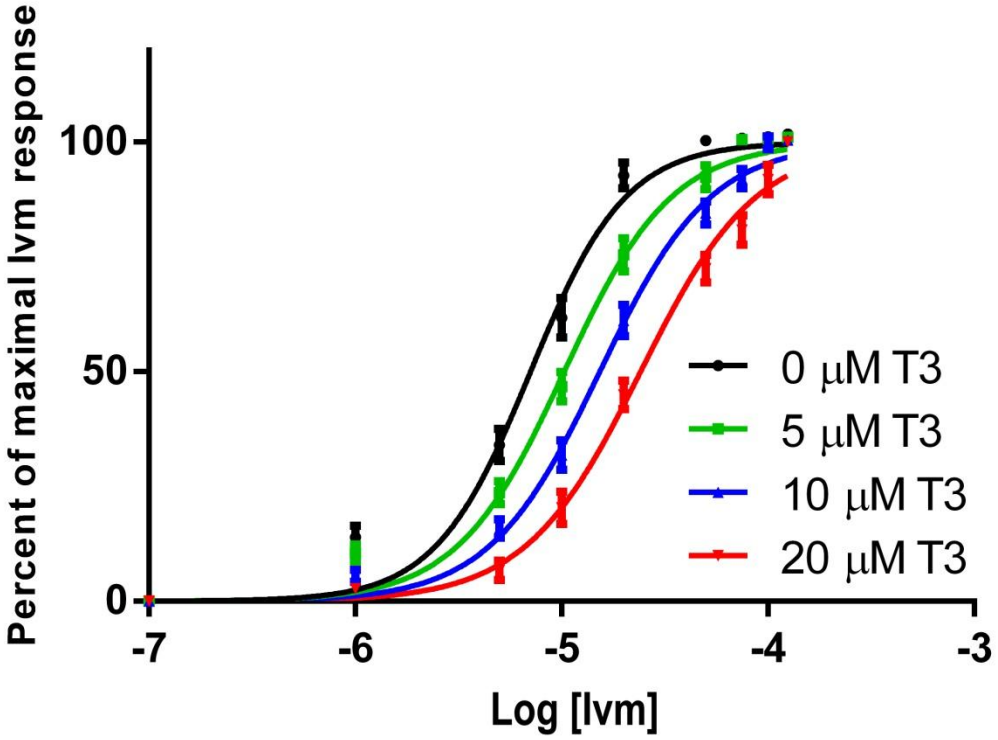

Figure 5. T3 competitive binding study against Ivermectin. Ivermectin concentration-response curves were taken in various steady concentrations of T3 (0 - 20 μM) to determine type of competition T3 exerts on ivermectin. Curves shift to the right with increasing concentrations of T3, but no changes in maximal response were observed. Results are represented as a percentage of the maximal ivermectin response without T3 presence (mean ± S.E.M., n =3).

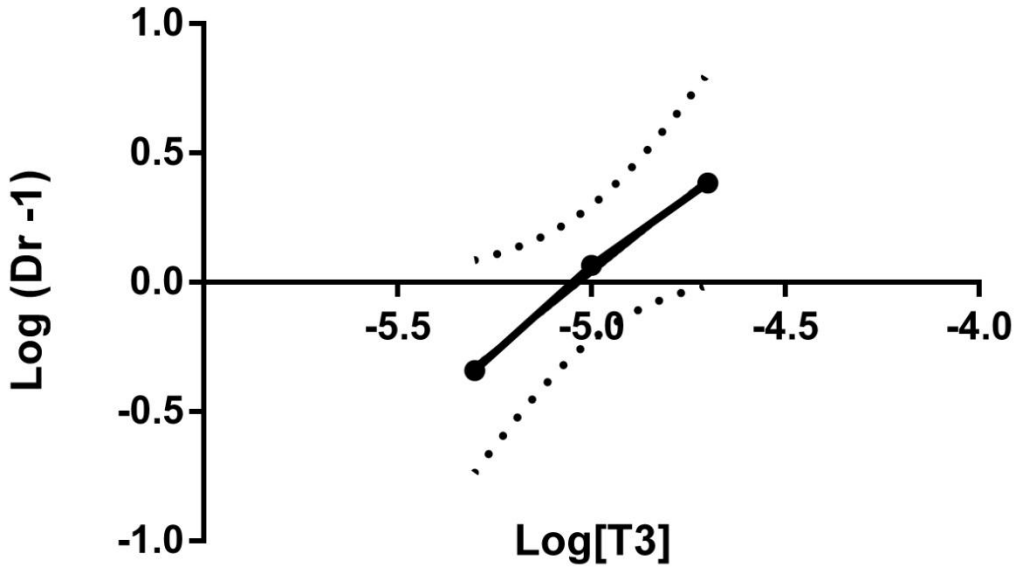

Figure 6. Schild plot of competitive binding study between T3 and Ivermectin. A Schild plot was taken from the competitive binding study to verify type of inhibition. Slope of 1.27 ± 0.03 was recorded with no significant difference from unity (slope of 1). A pA2 value of -5.060 ± .11 was calculated. The Dotted lines indicate 95% confidence intervals.

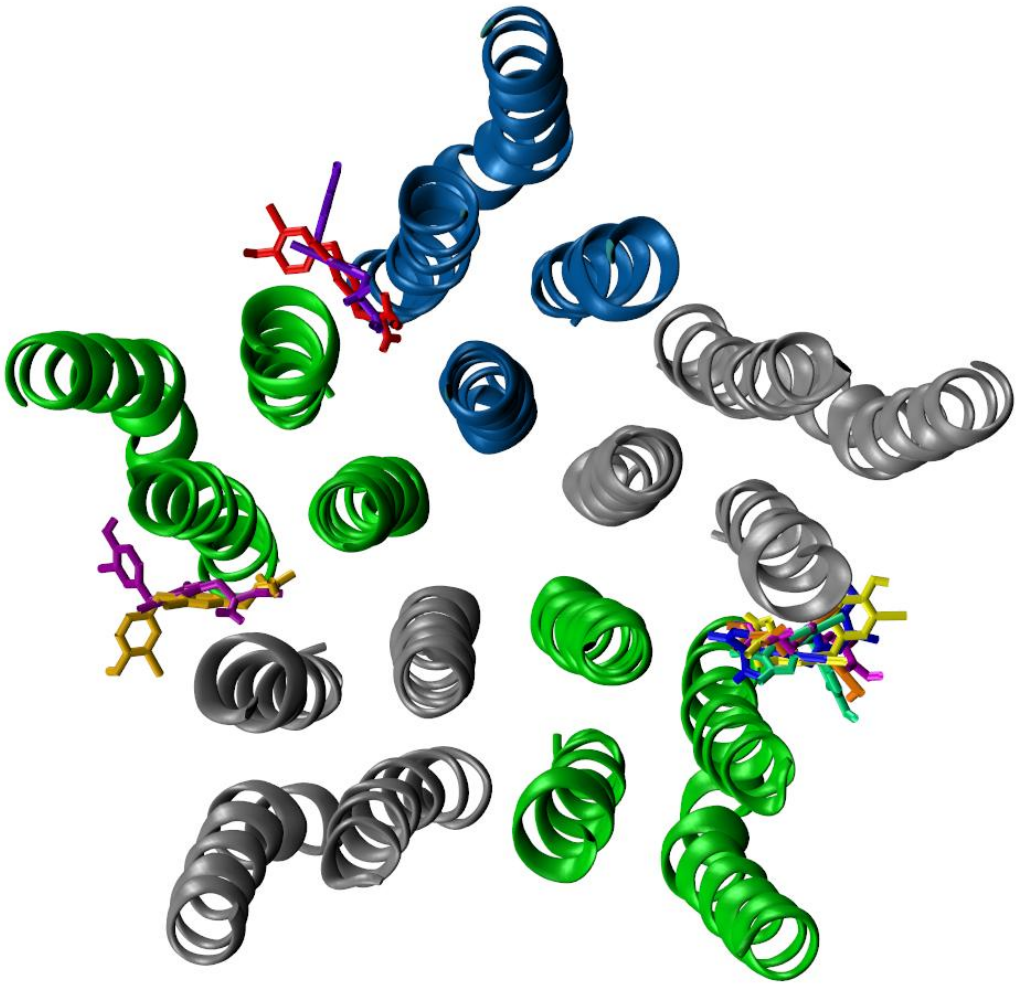

Figure 7. Molecular dynamics docking analysis of T3 on the $GABA_A$ receptor. An example visualization of the docking results taken from AutoDock Vina with possible binding modes found in the transmembrane domain. Subunits are represented as alpha (silver), beta (green), and gamma (blue). Calculated affinities (kcal/mol) were between -5.6 and -6.3.

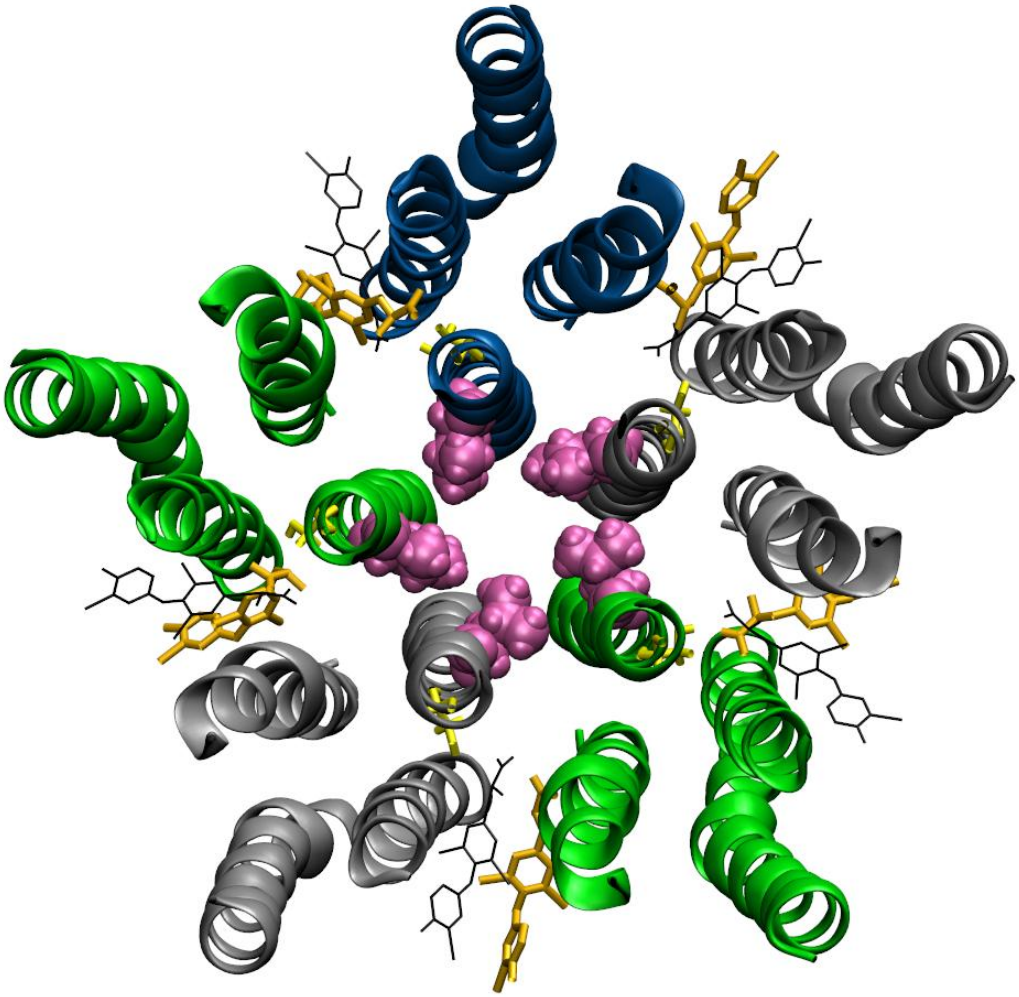

Figure 8. Representation of beginning and end coordinates of T3 in the transmembrane domain determined by molecular dynamics. Subunits are represented as alpha (silver), beta (green), and gamma (blue). The black representation of T3 indicates the beginning coordinates of the molecule, while the orange representation displays the end coordinates. The pink residues are the leucines that comprise the hydrophobic constriction. The yellow residues are the serines whose interactions with T3 were of interest to determining the mechanism of action.

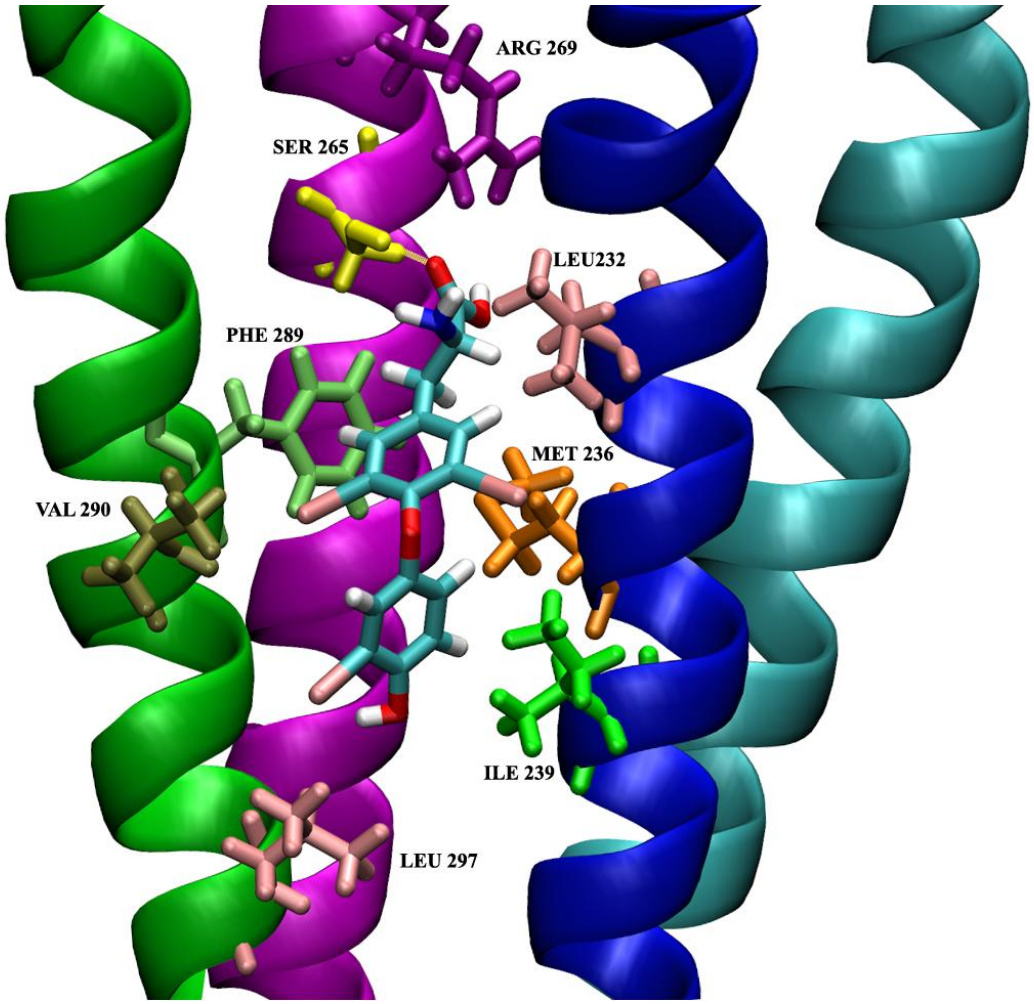

Figure 9. Representation of hydrogen bonding of T3 with serine residues. Sample frame showing T3 bound in between two subunits (alpha and beta in this representation). Alpha's M2 is cyan and M3 is blue, while Beta's M2 is purple and M1 is green. T3 is colored by atom type while the various amino acids that interact with T3 are displayed by residue type. Hydrogen bonds are represented by a yellow dashed line.

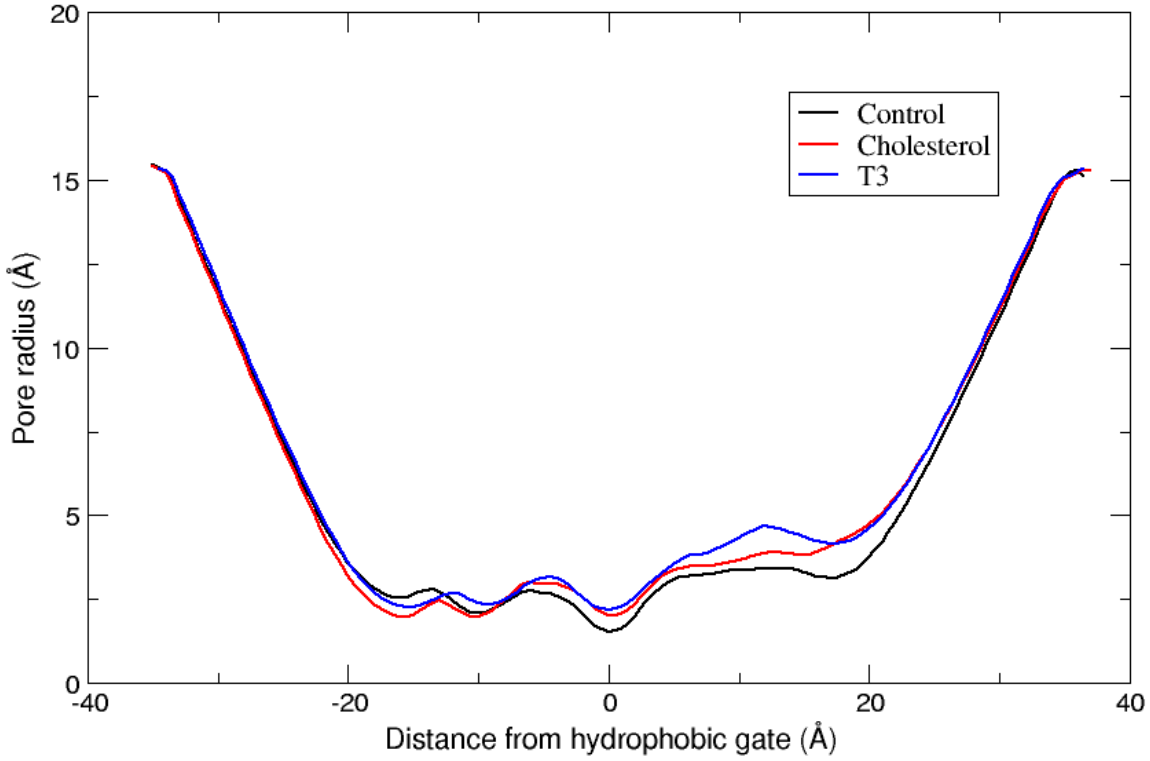

Figure 10. Pore radius plotted along longitudinal distance along the pore. A representation of the averaged pore radius through all frames (200 ns). The zero value is the hydrophobic gate, positive values represent towards the extracellular region, while negative values indicate towards the intracellular regions. The averaged pore radius was compared to a control simulation with no ligand bound to the transmembrane domain site, and a cholesterol-bound simulation. The profile of T3 is blue, cholesterol is red, and control is black. The averaged pore radius of T3 was ~1 Å larger than the control at the hydrophobic gate.

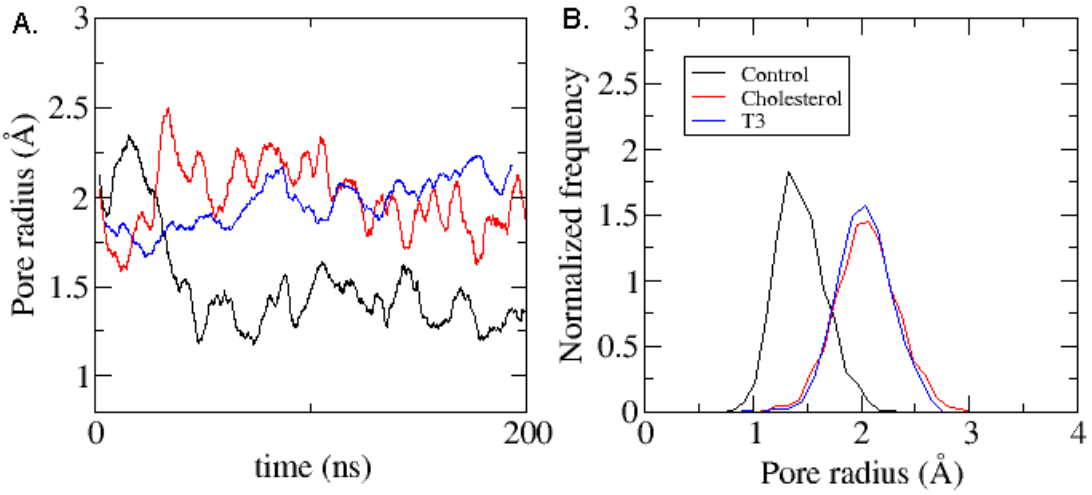

Figure 11. Pore radius timeline throughout simulation with histogram. A. A representation of the minimal pore radius throughout time. The profile of T3 is blue, cholesterol is red, and control is black. The minimal pore radius of T3 is significantly larger than the control, but similar to cholesterol. **B.** A histogram of the minimal pore radius. The peak of the minimal pore radius for T3 is ~2 Å, larger than the control, but similar to cholesterol. T3 and the control have a region of overlap, but a majority of the profile for T3 is larger.

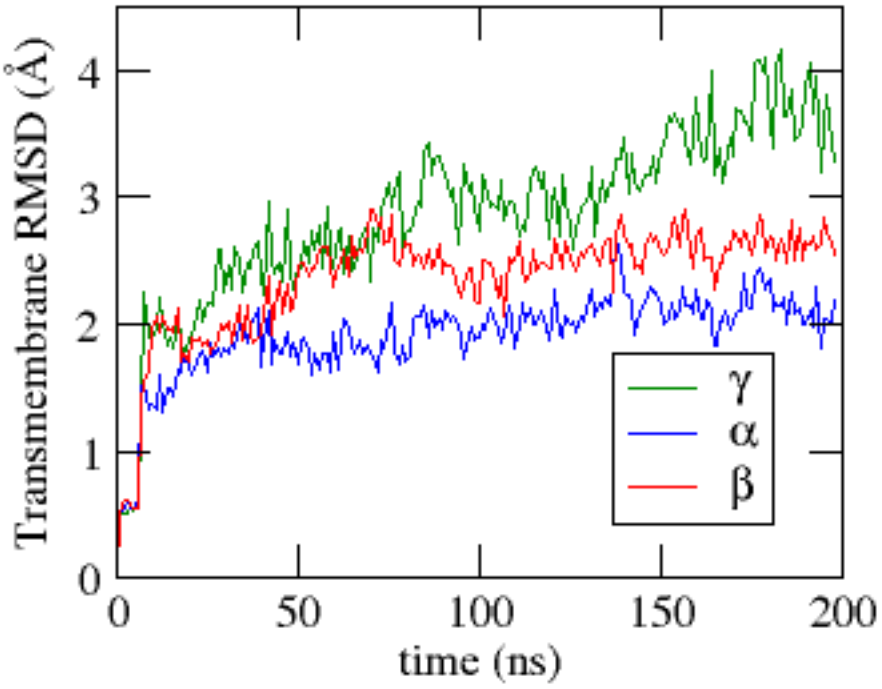

Figure 12. Root-mean squared deviation of subunits during the simulation. The root-mean squared deviation profile displays the movement of the subunits away from their initial coordinates. The RMSD of α (blue) and β (red) subunits increase within the first 50 ns but remain at a stable distance. The RMSD of the γ subunit increases throughout the simulation.

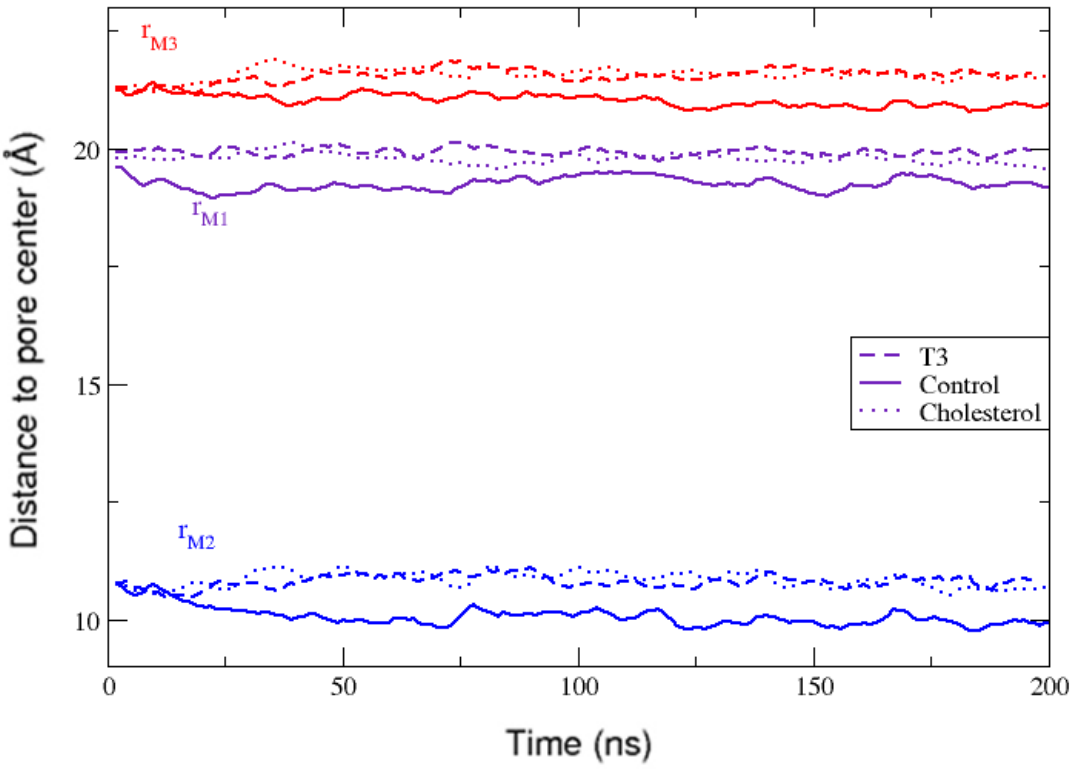

Figure 13. Distances of M1, M2, and M3 helices from the pore throughout the simulation. Changes in the individual alpha helices were analyzed to determine a possible wedge mechanism for the interaction of T3 on the receptor. The M1, M2, M3 distance from the pore center were compared across the simulation. In all helices, T3 (dashed line) helical distance was significantly greater than that of the control (solid line). T3 distances were also very similar to the cholesterol (dotted line).

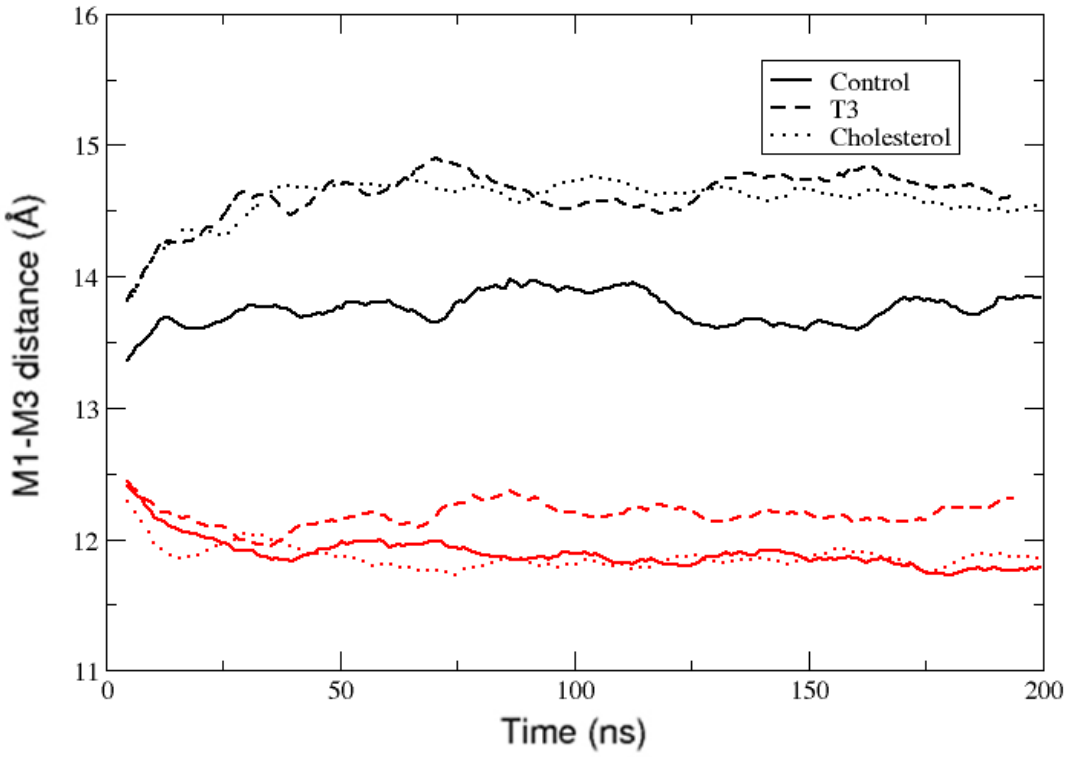

Figure 14. Distances of M1-M3 of same subunit and M3-M1 of adjacent subunits throughout the simulation. M3-M1 intersubunit distance (black) and M1-M3 intrasubunit distance (red) were analyzed for the possible wedge mechanism. The M3-M1 intersubunit distance of T3 (dashed line) was significantly larger than the control (solid line), but similar to the cholesterol (dotted line). The M1-M3 intrasubunit distance of T3 is not significantly greater than the control or cholesterol.

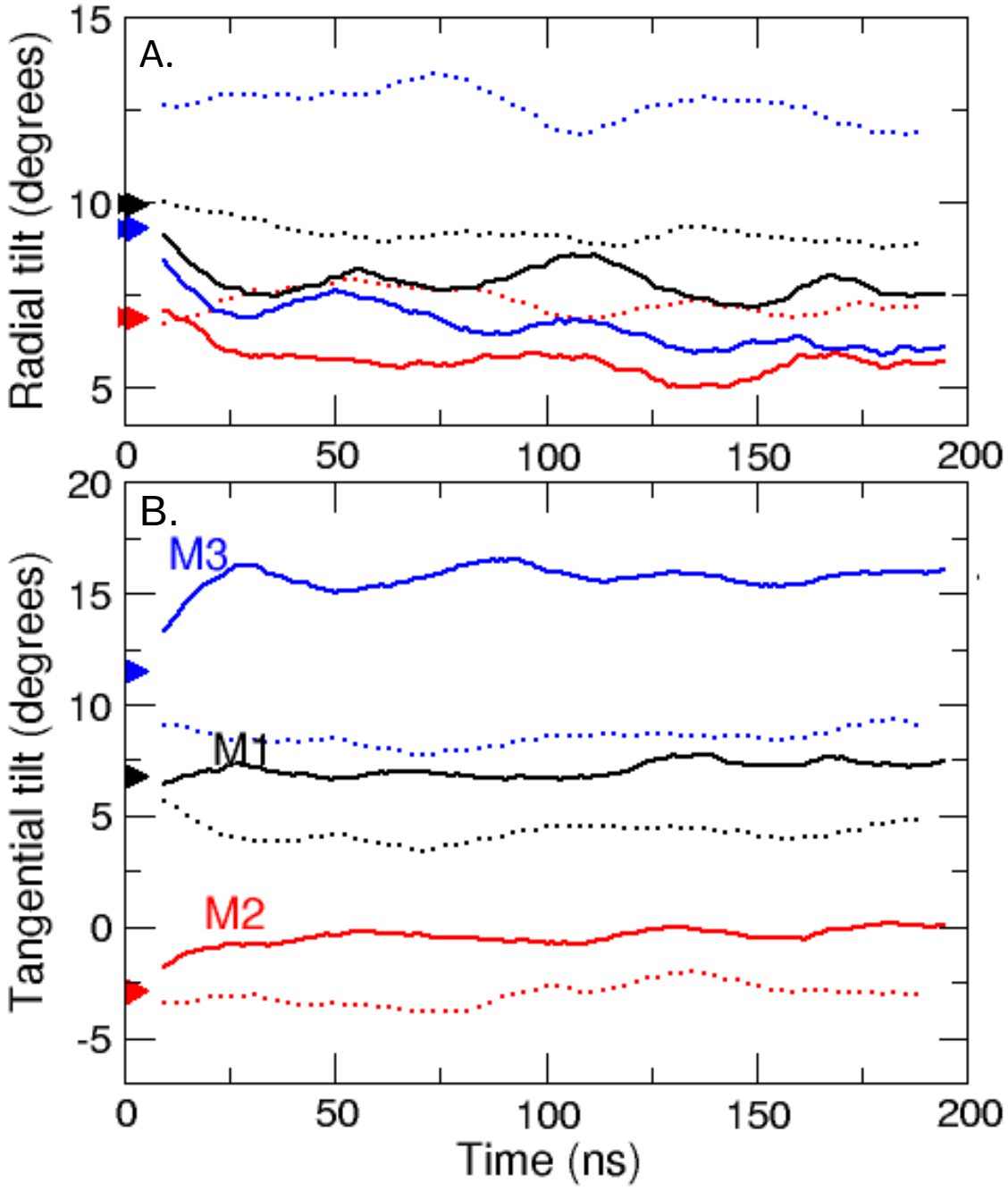

Figure 15. Helical tilt changes through the interaction of T3. A. Radial angle changes of the alpha helices were analyzed throughout the simulation. Radial tilt shows tilt towards or away from the pore. T3 radial tilt (dotted line) was significantly larger than control (solid line) in all helices, showing the greatest change in the M3 helix. **B.** Tangential angle changes of the alpha

helices represent the twisting of the helices. The tangential angles of T3 helices were significantly smaller than the control, with M3 showing the largest difference.

REFERENCES

Adelsberger, H., Scheuer, T., Dudel, J., 1997. A patch clamp study of a glutamatergic chloride channel on pharyngeal muscle of the nematode Ascaris suum. Neurosci. Lett. 230, 183–186.

Adelsberger, H., Lepier, A., Dudel, J., 2000. Activation of rat recombinant a1b1y2s GABAA receptor by the insecticide invermectin. Euro, J. of Pharm. 394, 163-170.

Akk, G., Covey, D.F., Evers, A.S., Steinbach, J.H., Zorumski, C.F., Mennerick, S., 2007. Mechanisms of neurosteroid interactions with GABAA receptors. Pharmacol. Ther. 116, 35—57.

Akk, G., Bracamontes, J., Steinbach, J.H., 2001. Pregnenolone sulfate block of GABAA receptors:mechanism and involvement of a residue in the M2 regious of the alpha subunit. J. of Phys. 532, 673-684.

Arena, J.P., 1994. Expression of Caenorhabditis elegans messenger RNA in Xenopus-oocytes: a model system to study the mechanism of action of avermectins. Parasitol. Today 10, 35–37.

Baumann, S.W., Baur, R., Sigel, E., 2002. Forced subunit assembly in α1β2γ2 GABAA receptors. J. of Bio. Chem. 277, 46020-46026.

Barker, J.L., Harrison, N.L., Lange, G.D., Owen, D.G., 1987. Potentiation of g-aminobutyric-acid-activated chloride conductance by a steroid anaesthetic in cultured rat spinal neurones. J. Physiol. 386, 485–501.

Baulieu E.E., 1991. Neurosteroids: a new function in the brain. Biol. Cell 71, 3 10.

Belelli, D., Casula, A., Ling, A., Lambert, J., 2002. The influence of subunit composition on the interaction of neurosteroids with GABAA receptors. Neuropharmacology 43, 651—661.

Bocquet N, et al., 2009. X-ray structure of a pentameric ligand-gated ion channel in an apparently open conformation. Nature 457,111–114.

Chapell, R., Martin, J.V., Machu, T.K., Leidenheimer, N.J., 1998. Direct channel-gating and modulatory effects of triiodothyronine on recombinant GABAA receptors. Euro. J. of Pharm. 349, 151-121.

Covey, D.F., Evers, A.S., Mennerick, S., Zorumski, C.F., Purdy, R.H., 2001. Recent developments in structure-activity relationships for steroid modulators of GABAA receptors. Brain Research Reviews 37, 91-97.

Dratman M.B., Crutchfield F.L., Axelrod J., Colburn R.W., Thoa N., 1976. Localization of triiodothyronine in nerve ending fractions of rat brain. Proc. nam. Acad. Sci. U.S.A. 73, 941 944.

Dratman M.B., Crutchfield F.L., Gordon J.T., Jennings A.S., 1983. Iodothyronine homeostasis in rat brain during hypo- and hyperthyroidism. Am. J. Physiol. 245, E189-E193.

Dratman, M.B., Gordon, J.T., 1996. Thyroid hormones as neurotransmitters. Thyroid 6, 639–647.

Eswar, N. et al., 2007. Comparative protein structure modeling using modeller. Curr. Protoc. Protein Sci. Chapter 2: Unit 2.9.

Gee K.W., 1988. Steroid modulation of the GABA/benzodiazepine receptor-linked chloride ionophore. Molec. Neurobiol. 2, 291-317.

Gee K.W., Bolger M.B., Brinton R.E., Coirini H., McEwen B. S., 1988. Steroid modulation of the chloride ionophore in rat brain: structure-activity requirements, regional dependence and mechanism of action. J. Pharmac. exp. Ther. 246, 803 8 i2.

Go T., Ito M., Okuno T., Mikawa H., 1988. Effect of thyroid hormones on benzodiazepine receptors in neuron-enriched primary cultures. J. Neurochem. 51, 1497-1500.

Grubmüller, H., Heymann, B., Tavan, P., 1996. Ligand binding: Molecular mechanics calculation of the streptavidin–biotin rupture force. Science 271, 997–999.

Hara, M., Yoshihisa, K., Ikemoto, Y., 1993. Propofol activates GABAA receptor–chloride ionophore complex in dissociated hippocampal pyramidal neurons of the rat. Anesthesiology 79, 781–788.

Hibbs, R.E. and Gouaux, E., 2011. Principles of activation and permeation in an anion-selective cys-loop receptor. Nature 474, 54-60.

Hilf, R.J.C. and Dutzle,r R., 2008. X-ray structure of a prokaryotic pentameric ligand-gated ion channel. Nature 452,375–379.

Hilf, R.J.C. and Dutzler, R., 2009. Structure of a potentially open state of a proton-activated pentameric ligand-gated ion channel. Nature 457,115–118.

Hill-Venning, C., Belelli, D., Peters, J., Lambert, J.J., 1997. Subunit-dependent interaction of the general anaesthetic etomidate with the γ -aminobutyric acid type A receptor. Br. J. Pharmacol. 120, 749–756.

Hosie, A.M., Wilkins, M.E., da Silva, H.M. Smart, T.G., 2006. Endogenous neurosteroids regulate GABAA receptors through two discrete transmembrane sites. Nature 444, 486-489.

Humphrey, W., Dalke, A., Schulten, K., 1996. VMD: visual molecular dynamics. J. Mol. Graph 14, 33-8.

Kragie L., 1993. Neuropsychiatric implications of thyroid hormone and benzodiazepine interactions. Endocr. Res. 19, 1-32.

Krasowski, M.D., Harrison, N.L., 1999. General anesthetic actions on ligand-gated ion channels. Cell. Mol. Life Sci. 55, 1278-1303.

Krsek, J. and Zemkov, H., 1994. Effect of ivermectin on gamma-aminobutyric acid induced chloride currents in mouse hippocampal embryonic neurones. Eur. J. of Pharm. 259, 121-128.

Lambert, J.J., Cooper, M.A., Simmons, C.J., Belelli, D., 2009. Neurosteroids: endogenous allosteric modulators of GABAA receptors. Psychneuroendo. 34S, S48-S58.

MacKerell, A.D., Feig, M., Brooks, C.L., 2004. Improved treatment of the protein backbone in empirical force fields. J. Am. Chem. Soc. 126, 698-9.

Majewska M.D., 1992. Neurosteroids: endogenous bimodal modulators of the GABA A receptor. Mechanism of action and physiological significance. Prog. Neurobiol. 38, 379 395.

Majewska M.D., Harrison N.L., Schwartz R.D., Barker J.L., Paul S. M., 1986. Steroid hormone metabolites are barbiturate-like modulators of the GABA receptor. Science 232, 1004 1007.

Mason, G.A., Walker, C.H., Prange, A.J., 1993. L-Triiodothyronine: is this peripheral hormone a central neurotransmitter?. Neuropsychopharmacology 8, 253–258.

Martin, J.V., Williams, D.B., Fitzgerald, R.M., Im, H.K., Vonvoigtlander, P.F., 1996. Thyroid hormonal modulation of the binding and activity of the GABAA receptor complex of brain. Neuroscience 73, 705–713.

Martin, R.J., Robertson, A.P., Bjorn, H., 1997. Target sites of anthelmintics. Parasitology 114, 111–124.

Medina J.H. and DeRobertis E., 1985. Benzodiazepine receptor and thyroid hormones: in vivo and in vitro modulation. J. Neurochem. 44, 1340-1344.

Mowrey, D., Cheng, M.H., Liu, L.T., Willenbring, D., Lu, X., Wymore, T., Xu, Y., Tang, P., 2013. Asymmetric ligand binding facilitates conformational transistions in petameric ligand-gated ion channels. J. of the Amer. Chem. Soc. 135, 2172-2180.

Nagy A. and Lajtha A., 1983. Thyroid hormones and derivatives inhibit flunitrazepam binding. J. Neurochem. 40, 414-417.

Narihara R., Hirouchi M., Ichida T., Kuriyama K., Roberts E., 1994. Effects of thyroxine and its related compounds on cerebral GABA receptors: inhibitory action on benzodiazepine recognition site in GABA A receptor complex. Neurochem. Int. 25, 451-454.

Park-Chung, M., Malayev, A., Purdy, R.H., Gibbs, T.T., Farb, D.H., 1999. Sulfated and unsulfated steroids modulate GABBA receptor function through distinct sites. Brain Research 830, 72–87.

Peters, J.A., Kirkness, E.F., Callachan, H., Lambert, J.L., Turner, A.J., 1988. Modulation of the GABAA receptor by depressant barbiturates and pregnane steroids. Br. J. Pharmacol. 94, 1257–1269.

Phillips, J.C. et al., 2005. Scalable molecular dynamics with NAMD. J. Comp. Chem. 26, 1781-1802.

Puia, G., Santi, M., Vicini, S., Pritchitt, D.B., Purdy, R.H., Paul, S.M., Seeburg, P.H., Costa, E., 1990. Neurosteroids act on recombinant human GABAA receptors. Neuron 4, 759–765.

Purdy R.H., Morrow A.L., Blinn J.R., Paul S.M., 1990. Synthesis, metabolism, and pharmacological activity of 3~-hydroxy steroids which potentiate GABA-receptor-mediated chloride ion uptake in rat cerebral cortical synaptoneurosomes. J. reed. Chem. 33, 1572 1581.

Rudolph, U., Möhler, H., 2006. Gaba-based therapeutic approaches: GABAA receptor subtype functions. Curr. Opin. Pharm. 6, 18-23.

Simmonds M.A., Turner J.P., Harrison N. L., 1984. Interactions of steroids with the GABA-A receptor complex. Neuropharmacology 23, 877-878.

Smart, O.S, Neduvelil, J.G., Wang, X., Wallace, B.A., Sansom, M.S., 1996. Hole: a program for the analysis of the pore dimensions of ion channel structural models. J. Mol. Graph 14, 354-60.

Tanaka K., Inada M., Ishii H., Naito K., Nishikawa M., Mashio Y., Imura H., 1981. Inner ring monodeiodination of thyroxine and 3,5,3'-L-triiodothyronine in rat brain. Endocrinology 109, 1619 1624.

Trott, O. and Olson, A.J., 2010. AutoDock Vina: improving the speed and accuracy of docking with a new scoring function, efficient optimization and multithreading. J. of Comp. Chem. 31, 455-461.